

Supporting Information

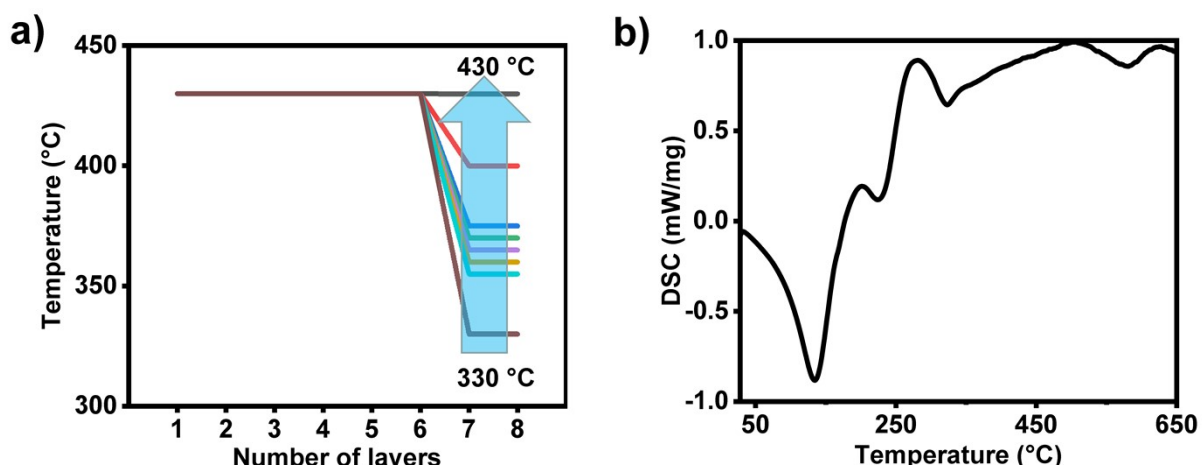


Fig. S1 Schematic diagram of the preparation of the precursor and the DSC curve of the precursor solution. (a) Schematic diagram of the relationship between the pre-annealing temperature and number of spin-coating layers. (b) The DSC curve of the precursor solution.

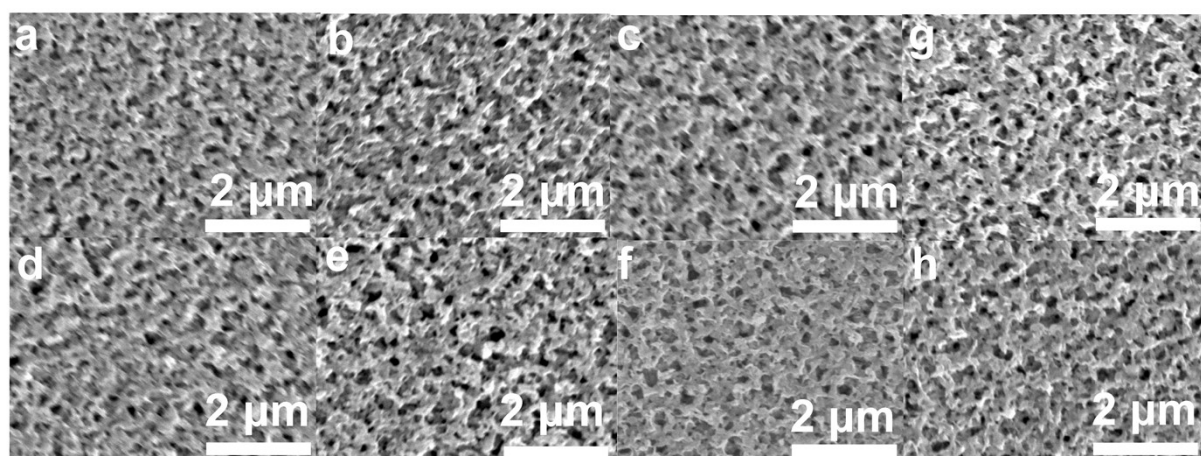


Fig. S2 Surface morphology of precursors with different spin-coating layers by SEM. a-h correspond to 1-8 layers of precursors, respectively, and the pre-annealing temperature of 7-8 layers is 365 °C. 1 layer for Mo back contact interface , while 8 layers for CdS frontier interface.

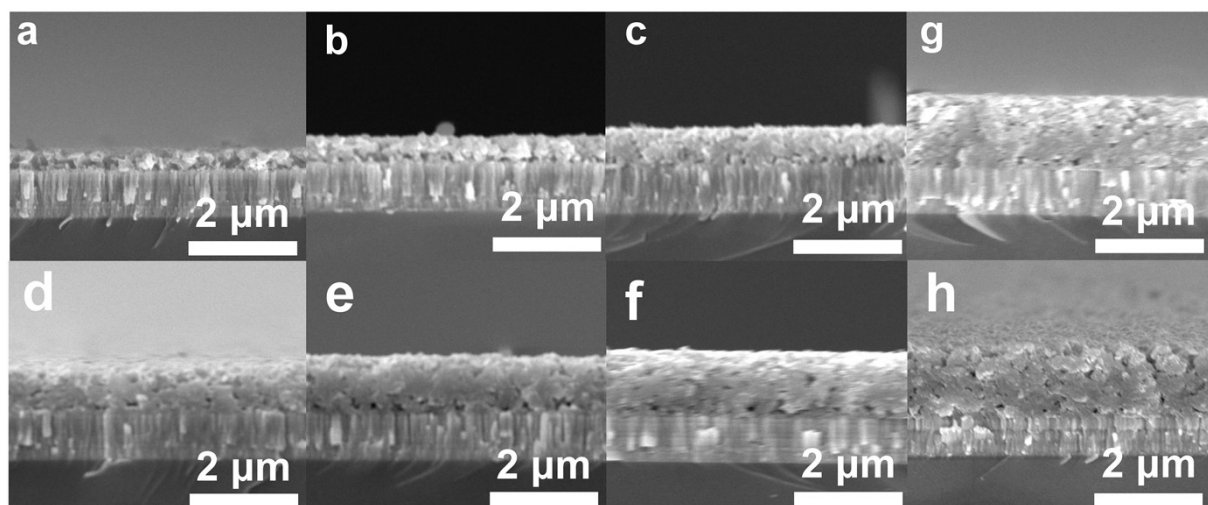


Fig. S3 SEM images of cross precursor films with different spin coating layers. a-h correspond to spin-coated 1-8 layers of precursor films, respectively. Pre-annealing temperature for 7-8 layers is at 365 °C. 1 layer for Mo back contact interface , while 8 layers

for CdS frontier interface.

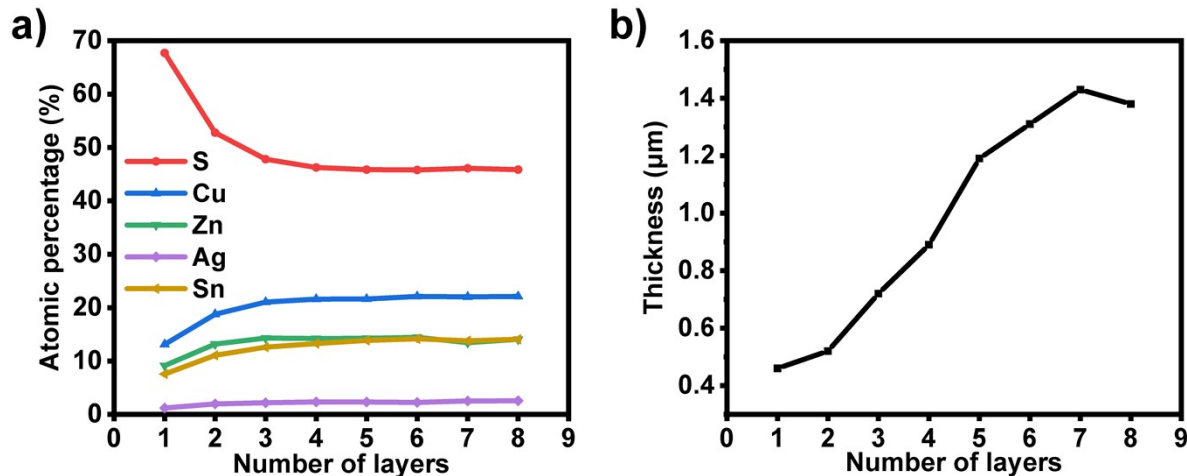


Fig. S4 The elemental contents and the thickness of precursors with different spin-coating layers. (a) the relationship between the thickness of the precursor film and spin coating layers. (b) The relationship between the distribution of metal elements in the precursor film and spin coating layers.

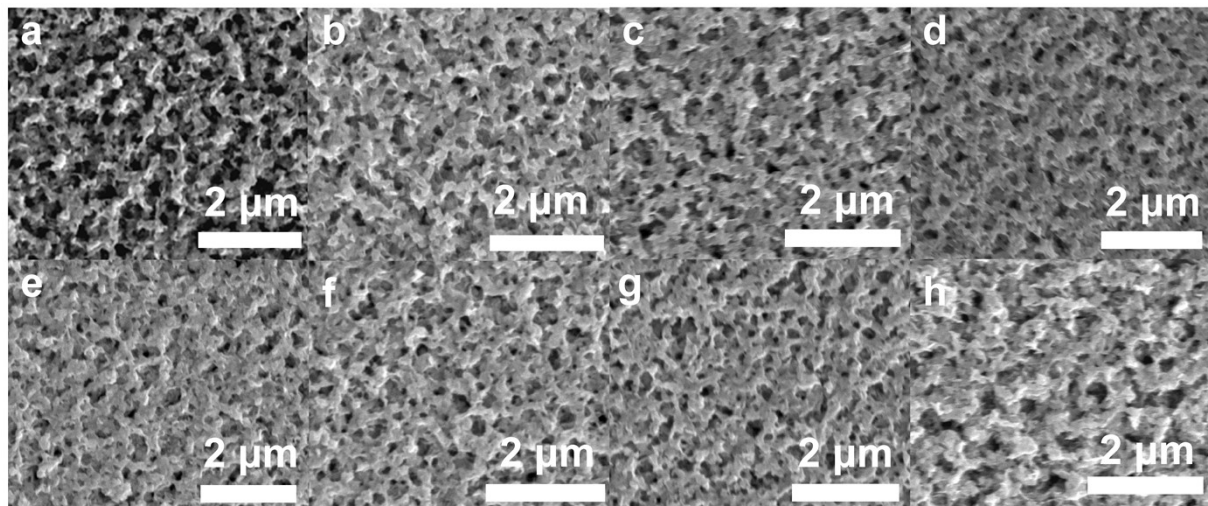


Figure. S5 Surface morphology of precursor films at different superficial pre-annealing temperature by SEM. (a) 330 °C (b) 355 °C (c) 360 °C (d) 365 °C (e) 370 °C (f) 375 °C (g) 400 °C (h) 430 °C.

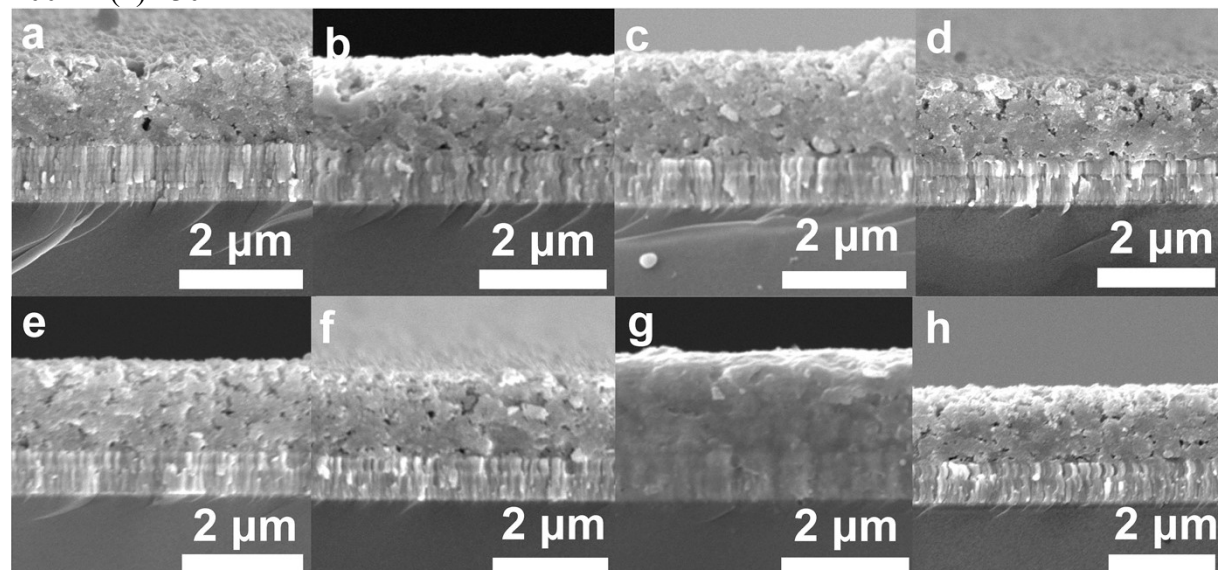


Fig. S6 Cross-section images of precursors with different superficial pre-annealing temperature by SEM. (a) 330 °C (b) 355 °C (c) 360 °C (d) 365 °C (e) 370 °C (f) 375 °C (g)

400 °C (h) 430 °C.

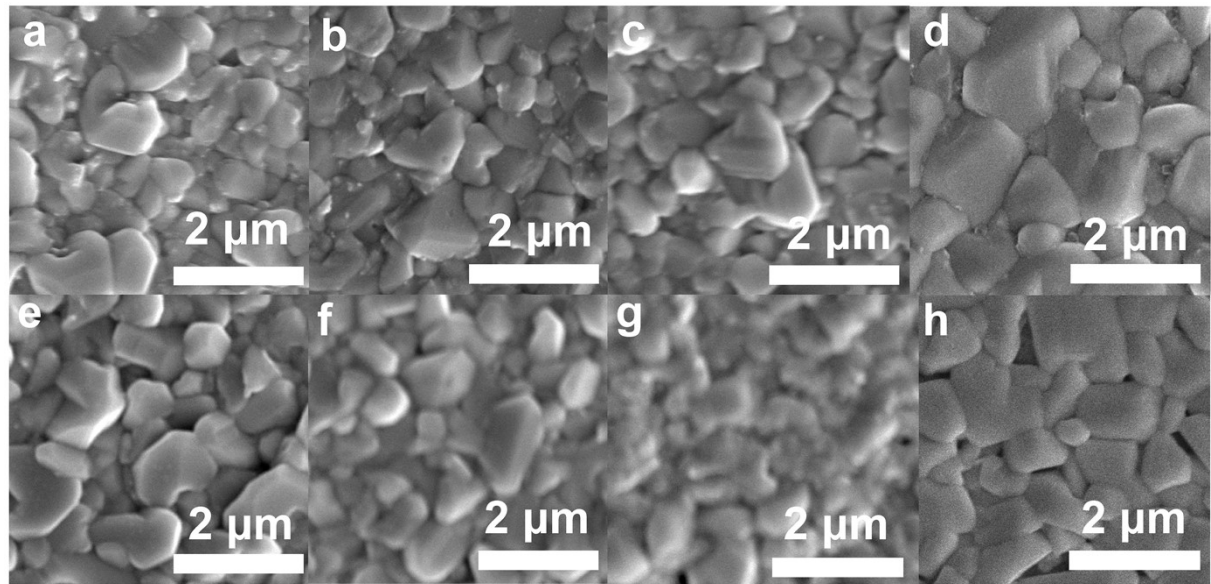


Fig. S7 Surface images of absorbers with different superficial pre-annealing temperature by SEM. (a) 330 °C (b) 355 °C (c) 360 °C (d) 365 °C (e) 370 °C (f) 375 °C (g) 400 °C (h) 430 °C.

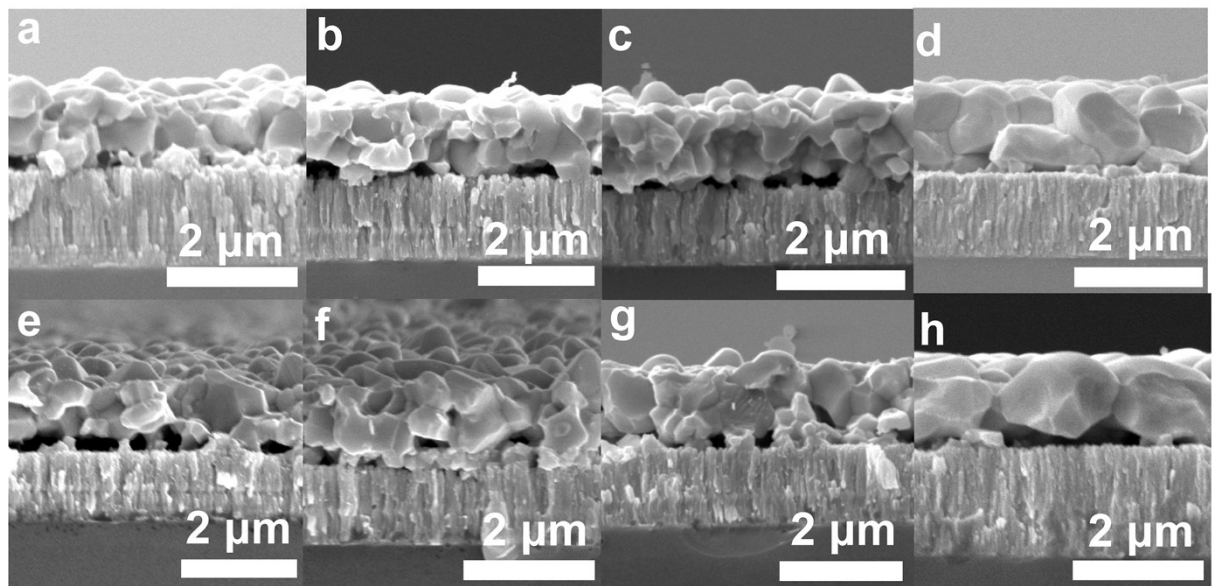


Fig. S8 Cross-section images of absorbers with different superficial pre-annealing temperature by SEM. (a) 330 °C (b) 355 °C (c) 360 °C (d) 365 °C (e) 370 °C (f) 375 °C (g) 400 °C (h) 430 °C.

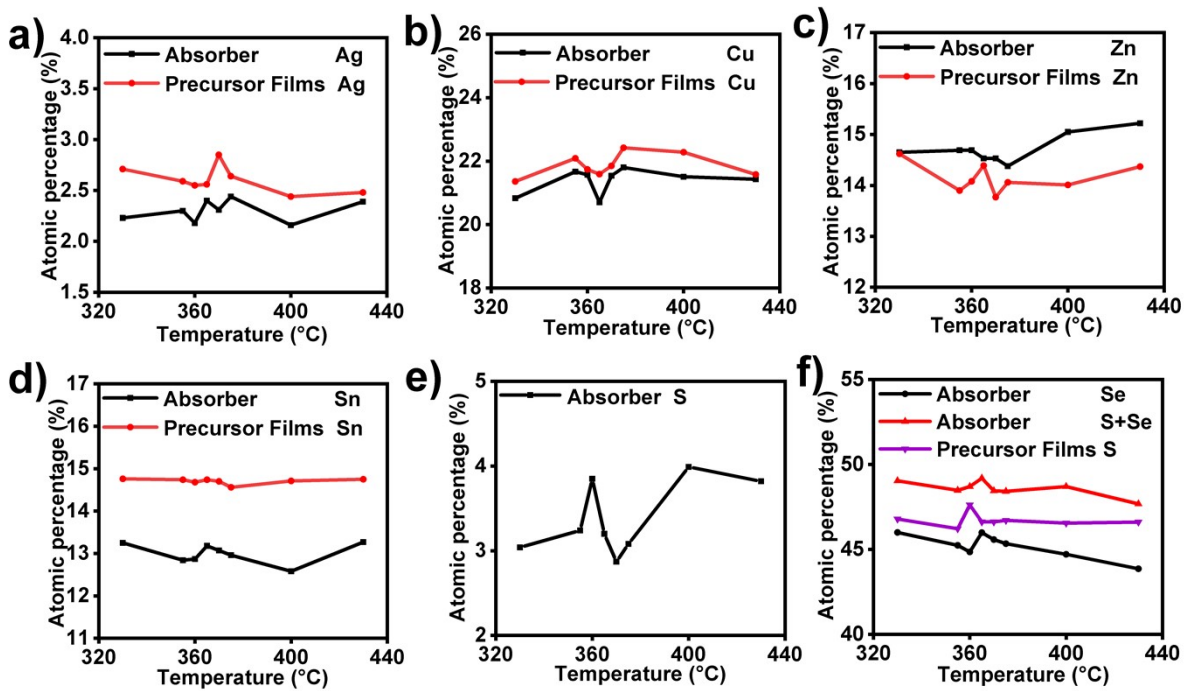


Fig. S9 Proportion of elements on the surface of precursors and absorbers with different superficial pre-annealing temperature (a) Ag (b) Cu (c) Zn (d) Sn (e) S in absorbers (f) S in precursors, Se and S+Se in absorbers, respectively.

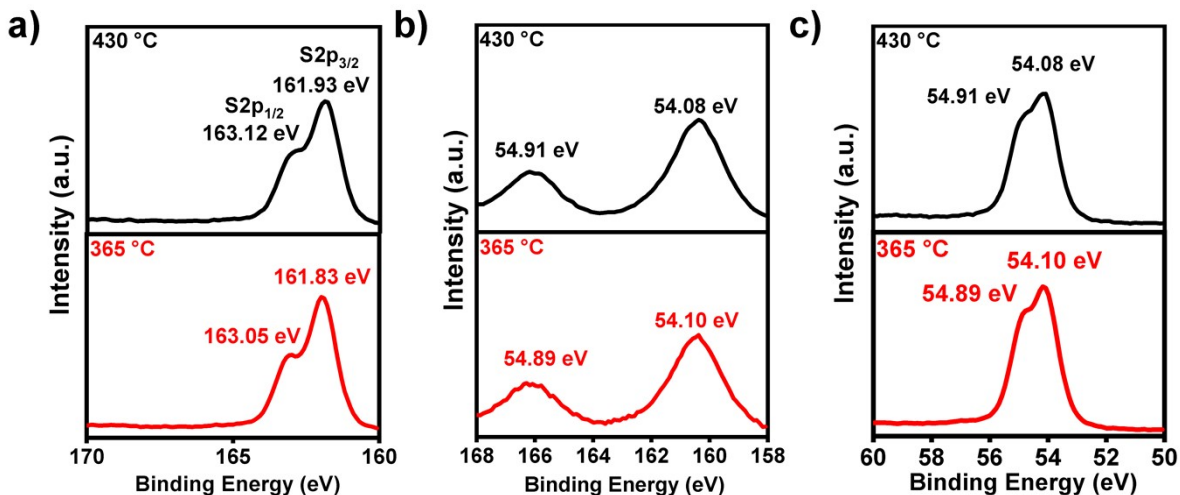


Fig. S10 XPS spectra of S and Se on the surface of precursors and absorbers with different superficial pre-annealing temperature (a) S in precursors, (b) S in absorbers, (c) Se in absorbers.

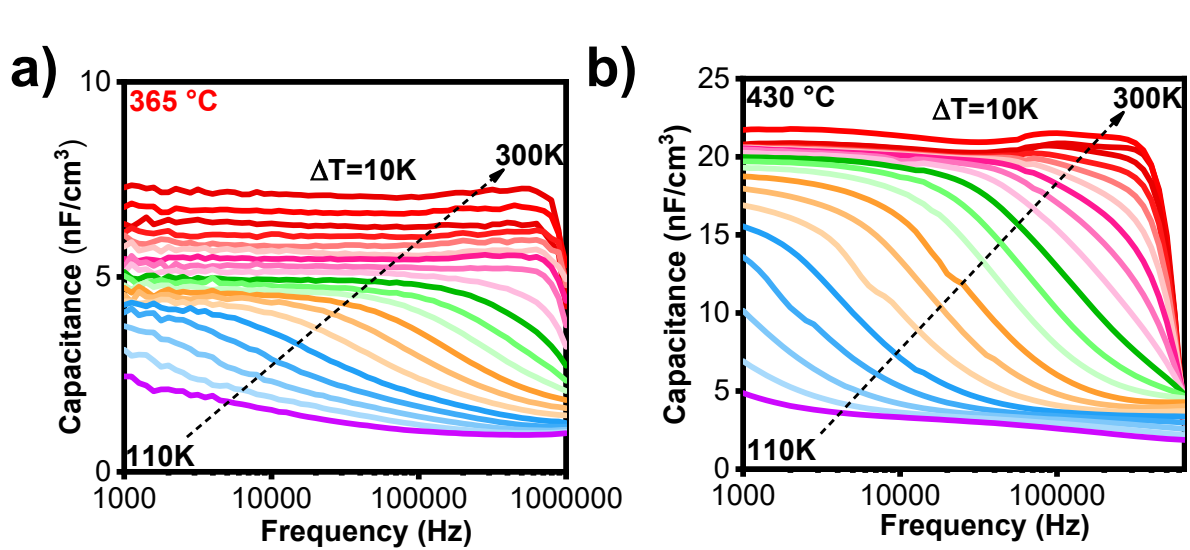
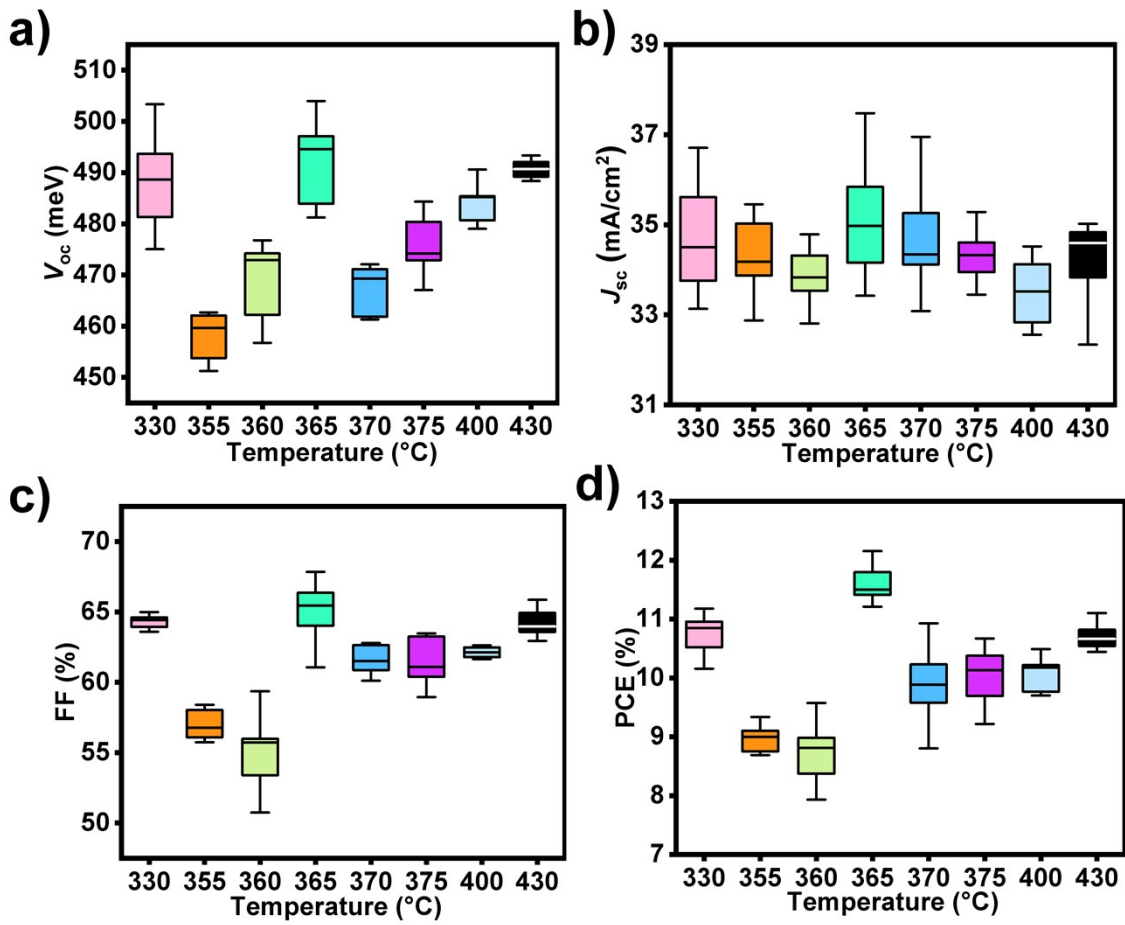


Table S1. Specific XRD parameters for (112) crystalline planes of CZTS precursors with different superficial pre-annealing temperature.

T (°C)	2-Theta (°)	β (°)	D (nm)	δ×10 ⁻³ (nm ⁻²)	ε×10 ⁻³
330	28.35772	1.47653	5.549436843	32.47148675	25.50037822
355	28.39196	1.40513	5.83186535	29.4025518	24.23676977
360	28.3898	1.36209	6.016114858	27.62916512	23.49624538
365	28.38513	1.40319	5.839840237	29.32230236	24.20937624
370	28.41211	1.20087	6.824130512	21.47362436	20.69822596
375	28.41211	1.20087	6.824130512	21.47362436	20.69822596
400	28.37032	1.30672	6.270767772	25.43071464	22.55723423
430	28.38344	1.15121	7.118053926	19.73683236	19.86317272

Table S2 Specific XRD parameters for (220) crystalline planes of CZTS precursors with different superficial pre-annealing temperature.

T (°C)	2-Theta (°)	β (°)	D (nm)	δ×10 ⁻³ (nm ⁻²)	ε×10 ⁻³
330	47.3523	1.8611	4.660908117	46.03190167	18.5201415
355	47.3523	1.86109	4.660933161	46.031407	18.52004198
360	47.41074	1.31175	6.61433763	22.85742379	13.03538033
365	47.41266	1.14028	7.609026922	17.27196537	11.33089914
370	47.38752	1.18173	7.341427973	18.55405824	11.74978726
375	47.402	1.04032	8.339805885	14.3776569	10.34021506
400	47.379	1.28633	6.744227876	21.98545855	12.79239609
430	47.38695	1.27531	6.802712079	21.60905724	12.6804124

Table S3 Specific XRD parameters for (112) crystalline planes of CZTSSe absorbers with different superficial pre-annealing temperature.

T (°C)	2-Theta (°)	β (°)	D (nm)	δ×10 ⁻³ (nm ⁻²)	ε×10 ⁻³
330	27.1322	0.17699	46.17377502	0.469039302	3.200443205
355	27.16279	0.19489	41.93556971	0.568636725	3.520000097
360	27.16279	0.19489	41.93556971	0.568636725	3.520000097
365	27.16701	0.1692	48.30316724	0.428596661	3.055508697
370	27.17732	0.19594	41.71212414	0.574745245	3.537000066
375	27.18941	0.2029	40.28231684	0.616270129	3.660947385
400	27.12773	0.1772	46.11862035	0.47016185	3.204788798
430	27.11854	0.17479	46.75359824	0.457477689	3.16231459

Table S4 Specific XRD parameters for (204) crystalline planes of CZTSSe absorbers with different superficial pre-annealing temperature.

T (°C)	2-Theta	β (°)	D (nm)	δ×10 ⁻³ (nm ⁻²)	ε×10 ⁻³
330	45.11925	0.34857	24.67954578	1.641820505	3.661053613
355	45.14665	0.37958	22.66558862	1.946551936	3.984064559
360	45.17205	0.37836	22.74076853	1.933702793	3.968777392
365	45.14769	0.34277	25.09973624	1.587309753	3.597615374
370	45.16474	0.39359	21.86023244	2.092620372	4.129274076
375	45.17855	0.38303	22.46403733	1.981638246	4.017120404
400	45.1128	0.35581	24.1768026	1.710811934	3.737689613

430	45.09938	0.34908	24.64171467	1.646865574	3.668205367
-----	----------	---------	-------------	-------------	-------------

Table S5 Specific XRD parameters for (312) crystalline planes of CZTSSe absorbers with different superficial pre-annealing temperature.

T (°C)	2-Theta	β (°)	D (nm)	δ×10 ⁻³ (nm ⁻²)	ε × 10 ⁻³
330	53.46361	0.5805	15.32294015	4.25907992	5.029172424
355	53.51116	0.74819	11.89115609	7.072156135	6.475206344
360	53.53557	0.68302	13.02711873	5.892549741	5.908118272
365	53.49667	0.66999	13.27819785	5.67181072	5.800304681
370	53.52912	0.68019	13.08094801	5.844152784	5.884462462
375	53.53635	0.58837	15.12281929	4.372546882	5.089310277
400	53.46	0.54127	16.43325075	3.702994235	4.689670342
430	53.44005	0.57302	15.52135349	4.150886138	4.966910979

Table S6 Proportion of metallic elements in precursors with different superficial annealing temperature via SEM EDX.

T (°C)	Cu/Ag	Cu+Ag/Zn+Sn	Zn/Sn
330	7.88	0.82	0.99
355	8.53	0.86	0.94
360	8.53	0.84	0.96
365	8.43	0.83	0.98
370	7.67	0.87	0.94
375	8.49	0.88	0.97
400	9.13	0.86	0.97
430	8.70	0.83	0.97

Table S7 Proportion of metallic elements in the absorbers pre-annealed at different superficial temperatures via SEM EDX.

T (°C)	Cu/Ag	Cu+Ag/Zn+Sn	Zn/Sn
330	9.34	0.83	1.11
355	9.42	0.87	1.14
360	9.89	0.86	1.14
365	8.63	0.83	1.10
370	9.32	0.86	1.11
375	8.93	0.89	1.11
400	9.95	0.84	1.15
430	8.96	0.84	1.15

Supplementary Note 1. The Grain size (D), dislocation density (δ) and residual stress (ε) were calculated by Debye-Scherrer formula, and the Debye-Scherrer formula was shown in Equation S1

$$D = \frac{K\gamma}{\beta \cos \theta} \quad (\text{S1})$$

K ($K=0.89$) is the Scherrer constant, γ is the X-ray wavelength (1.54056 Å for Cu $\text{k}\alpha$), β is the full width at half maximum the diffraction peak of the measured sample, which needs to be converted into radians (rad) in the process of calculation, θ is the Bragg diffraction angle.

Supplementary Note 2. The admittance spectra were plotted by capacitance (C) vs. frequency (f), and the inflection frequency f_0 for each AS curve at different temperatures was determined by the maximum point of $-f \frac{dC}{df}$ vs. frequency. According to inflection angular frequency $\omega_0 = 2\pi f_0$ and Equation S2, we obtained Equation S3. then the Arrhenius plots of $\ln \omega_0/T^2$ vs. $1000/T$ were obtained.

$$\omega_0 = 2\pi\nu_0 T^2 \exp\left(\frac{-E_a}{kT}\right) \quad (\text{S2})$$

$$\ln\left(\frac{\omega_0}{T^2}\right) = -\frac{E_a}{kT} + \ln(2\pi\nu_0) \quad (\text{S3})$$

E_a was derived from the slope of the Arrhenius plots, and ν_0 was extracted from the y-axis intercept $\ln(2\pi\nu_0)$. Subsequently, to obtain energy distribution of defects, the energy as a function of angular frequency was presented in Equation S4:

$$E(\omega) = kT \ln\left(\frac{2\pi\nu_0 T^2}{\omega}\right) \quad (\text{S4})$$

And differential capacitance spectrum reflecting defect concentration at each temperature was superimposed, following Equation S5:

$$N_t[E(\omega)] = -\frac{V_{bi}}{qWkT} \omega \frac{dC}{d\omega} \quad (\text{S5})$$

The V_{bi} is built-in potential, which was extracted from the plots of $1/C^2$ vs. V . W is the depletion region width of the junction, which were extracted from the plots of N_{CV} vs. X . Normally, the values of E_a and $E(\omega)_0$ corresponding to the peak of N_t curve should be similar, which are the energy level of defects relative to the valence band maximum (VBM). The values of defect density (N_t) were obtained from the integral peak areas of N_t curve via Gaussian fitting.